

DOI: <https://doi.org/10.15407/kvt188.02.005>

UDC 616.12

**K.B. ORIKHOVSKA**, Postgraduate student,  
Junior Researcher of the Department of Intelligent Automatic Systems  
e-mail: kseniaor@gmail.com

**L.S. FAINZILBERG**, Dr (Engineering), Associate Professor (Docent),  
Chief Researcher of Data Processing Department  
e-mail: fainzilberg@gmail.com  
International Research and Training Center for Information Technologies and Systems  
of the NAS of Ukraine and Ministry of Education and Science of Ukraine,  
Acad. Glushkova av., 40, Kiev, 03680, Ukraine

## COMPARATIVE ANALYSIS OF ESTIMATION METHODS OF THE PHYSIOLOGICAL SIGNALS VARIABILITY

---

*Introduction.* In the modern world, more attention is paid to the study of the behavior of complexly organized medical and biological systems. The fundamental concept of synergetics is the generalized entropy, which quantitatively characterizes the degree of the system chaoticness. Of special interest are studies of changes in the dynamic series chaotic parameters generated by various biological systems.

*The purpose of the article is further development and experimental research of methods for analyzing the variability of physiological signals under external influences on the body.*

*Methods.* Two alternative approaches of estimating the variability of dynamic series are investigated: based on the calculation of the sample variance relative changes and entropy estimates (in a sliding window with the specified parameters) in relation to the first window. The theoretical and experimental dependences between the Shannon entropy and the standard deviation for a normal distribution of a random variable that generates a dynamic series are studied. Comparison of these estimates with real and model data is carried out.

*Results.* To increase the sensitivity of entropy estimates to the variability of the dynamic series, it is proposed to move from a series of discrete entropy  $h(l)$  values at the  $l$ -th point, calculated by the sliding window method, to its phase portrait on the plane  $h(l), \dot{h}(l)$ , where  $\dot{h}(l)$  is the estimate of the first derivative  $h(l)$ . For an integral assessment of the chaotic nature of physiological signals, it is suggested to estimate the area of the convex hull of the entropy phase portrait and the coordinates of the phase portrait gravity center  $X, Y$ . Experimental studies have confirmed the diagnostic value of these parameters in the assessment of variability of the electrocardiograms and rhythmograms indices with external influences

on the body (intravenous therapy, surgery and physical activity).

*Conclusions.* Deviations of the integral parameters of the entropy phase portrait under the effect of external influences on the organism were detected, which open new possibilities in the evaluation of the cardiac activity regulation in preventive and clinical medicine. These integral parameters require further study to confirm their statistical significance in representative samples of observations.

**Keywords:** variability of physiological signals, entropy estimates, diagnostic criteria.

## INTRODUCTION

In the modern world more attention is paid to the behavior of complexly organized medical and biological systems [1]. For this purpose synergetic methods are used, aimed at studying the general laws of processes in nonlinear dynamical systems and the research of the relationship between ordered and chaotic structures [2].

The fundamental concept of synergetics is the generalized entropy, which quantitatively characterizes the degree of system chaoticness. In cardiology, entropic indices are actively studied to assess the heart rhythm chaoticness. For example, in [3–5], the relationship between entropy and traditional heart rate parameters was studied. It was found that in healthy people the RR-intervals entropy correlates reliably with all the main indicators of heart rate variability (HRV).

Interesting results were obtained by analyzing the relationship between the traditional HRV parameters and the sample entropy under isometric and dynamic loads [6]. Studies have shown that in healthy volunteers the traditional HRV parameters react equally to both types of load, while the sample entropy significantly changed only under isometric load. This indicates that the vegetative control of cardiovascular reactions to isometric and dynamic loads is different. It allows us to change the traditional view on the interaction between the branches of the autonomic nervous system.

Changes in the chaoticness of the different dynamic series parameters, which carry additional diagnostic value, for example, in the rhythmogram [7, 8] or the electroencephalogram [9], are of particular interest.

There are different approaches to solve such problems. The simplest way is to estimate the entropy calculated from successive sections of the dynamic series (windows) and compare the estimates that are normalized by the first window. Based on such studies, it was possible to detect gender differences in the time variation of Shannon entropy of the conditionally healthy men and women electrocardiograms (ECG) in response to stressful effects [10].

In the process of research, another curious fact was established, which, in the author's opinion [10], is worth a special study. It has been found that the most stable parameter, reflecting statistically significant changes in the signal over time, is precisely entropy, and not dispersion.

According to [11], important information about the properties of the system carries not only by the entropy itself, but also by the nature changes over time. In [12], a number of interesting results on the entropy method usage were obtained for a comprehensive assessment of the risk factors dynamics for cardiovascular diseases.

Since mathematical methods for estimating the variability of dynamic series

are becoming increasingly popular in the solution of applied problems, it is necessary to carry out additional studies and determine the conditions under which the analysis of Shannon and other entropies will be more effective.

The purpose of the article is further development and experimental research of methods for analyzing the variability of physiological signals under external influences on the body.

## TWO APPROACHES TO ESTIMATION OF DYNAMIC RANGE VARIABILITY

Let it be required to evaluate experimentally the variability of a values sequence

$$A = a_1, a_2, \dots, a_N, \quad (1)$$

representing the realization of some random variable  $X$  with an unknown distribution law  $p(X)$ .

This can be done if we calculate the sample variance

$$\sigma^2 = \frac{1}{N-1} \sum_{i=1}^N \left( a_i - \frac{1}{N} \sum_{i=1}^N a_i \right)^2, \quad (2)$$

which estimates the square of the values  $X$  deviations relative to the estimation of mathematical expectation  $M\{X\}$ .

The sample variance  $\sigma^2$  can be calculated as data is accumulated using the recursion formula, and with a minor modification such an estimate will be unbiased and consistent [13].

The second way of calculating the variability of the sequence (1) is based on the use of the statistical analogue of the well-known Shannon entropy expression

$$H = - \sum_{j=1}^n p_j \log_2 p_j, \quad (3)$$

where  $p_j$  is the frequency of entry values  $a_i$ ,  $i=1, \dots, N$  into the intervals  $\Delta_j = [a_j^-, a_j^+]$ ,  $j=1, \dots, n$ .

For a given  $n$  boundary  $a_j^-, a_j^+$  of these intervals, including those with alternating variables  $a_i$ , are determined by the relations

$$a_j^- = \min a_i + \frac{\max a_i - \min a_i}{n} (j-1), \quad j=1, \dots, n, \quad (4)$$

$$a_j^+ = \min a_i + \frac{\max a_i - \min a_i}{n} j, \quad j=1, \dots, n. \quad (5)$$

The greater the value  $H$ , the further the system is from the ordered state. The maximum value Shannon's entropy reaches when all states of the system are equally possible. It follows that the entropy (3) takes values on the interval  $[0, \log_2 n]$ . For convenience, instead of (3), the normalized entropy is often used

$$H_{norm} = \frac{\sum_{j=1}^n p_j \log_2 p_j}{\log_2 n} \in [0, 1]. \quad (6)$$

It is easy to show [14] that the value (3) is invariant under permutations of the series elements (1). Therefore, the Shannon entropy (3) itself, as well as dispersion (2), characterizes only the properties of the random variable  $X$  that generates the sequence (1), and not the variability of the sequence itself. Therefore, it is possible to estimate the variability of a dynamic series only by calculating (2) or (3) on individual sections of the processed sequence (1).

This can be done if you scan the observed time series with a sequence of windows, in each of which calculate the relative increment of entropy

$$H_l = \frac{-\sum_{j=1}^n p_{jl} \log p_{jl}}{H_1} \cdot 100 \%, \quad l=1, \dots, M, \quad (7)$$

where  $p_{jl}$  is the frequency of occurrence of the time series values, observed on the  $l$ -th fragment, the  $j$ -th interval  $\Delta_j = [a_j^-, a_j^+]$ ,  $j=1, \dots, n$ , and

$$H_1 = -\sum_{j=1}^n p_{j1} \log p_{j1} \quad (8)$$

is an entropy calculated in the first window, provided that  $H_1 \neq 0$ .

There are other entropy estimates of the dynamic series chaoticness, a comparative analysis of which is presented in [14]. For example, it is possible to calculate in each  $l$ -th window a modernized permutation entropy  $PE$ , which is based on estimating the frequency of five characteristic patterns appearance (Fig. 1).

Patterns classes are uniquely determined by the values  $a_i$ ,  $i=2, \dots, N-1$  of the sequence (1) as follows:

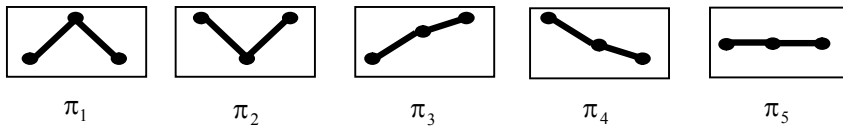
class  $\pi_1$ , if  $(a_i - a_{i-1}) > h \wedge (a_i - a_{i+1}) > h$ ,

class  $\pi_2$ , if  $(a_{i-1} - a_i) > h \wedge (a_{i+1} - a_i) > h$ ,

class  $\pi_3$ , if  $(a_i - a_{i-1}) > h \vee (a_{i+1} - a_i) > h \vee (a_{i+1} - a_{i-1}) > h$ ,

class  $\pi_4$ , if  $(a_{i-1} - a_i) > h \vee (a_i - a_{i+1}) > h \vee (a_{i-1} - a_{i+1}) > h$ ,

class  $\pi_5$ , if none of the above relations holds, in which  $h$  is a given threshold of insensitivity to local changes in the signal.



**Fig. 1.** Five classes of modernized permutation entropy patterns

Then the permutation entropy in the  $l$ -th window is calculated by the formula

$$PE_l = \frac{-\sum_{j=1}^5 p(\pi_{jl}) \log p(\pi_{jl})}{PE_1} \cdot 100\%, \quad l=1, \dots, M, \quad (9)$$

in which  $p(\pi_j)$  is the frequency of the pattern  $j$  appearance in the  $l$ -th window, and

$$PE_1 = -\sum_{j=1}^5 p(\pi_{j1}) \log p(\pi_{j1}) \quad (10)$$

is a permutation entropy calculated in the first window, provided that  $PE_1 \neq 0$ .

Similarly, one can get an idea of the dynamic series variability if one evaluates the variances (2) on successive signal windows of length  $K_0$ :

$$\sigma_l^2 = \frac{\frac{1}{K_0-1} \sum_{i=1}^{K_0} \left( a_{il} - \frac{1}{K_0} \sum_{i=1}^{K_0} a_{il} \right)^2}{\sigma_1^2} \cdot 100\%, \quad l=1, \dots, M, \quad (11)$$

where  $a_{il}$  are the discrete values observed in the  $l$ -th window, and

$$\sigma_1^2 = \frac{1}{K_0-1} \sum_{i=1}^{K_0} \left( a_{i1} - \frac{1}{K_0} \sum_{i=1}^{K_0} a_{i1} \right)^2 \quad (12)$$

is a variance estimation of the values  $a_{i1}$  observed in the first window under the assumption that  $\sigma_1^2 \neq 0$ .

Note that the procedures (7), (9) and (11) can be implemented when the  $l+1$ -th window is shifted by the  $l+1$ -th ratio to the  $K_0$  window width or when windows are shifted by one point (sliding window mode). It is clear that in the latter case the amount of necessary calculations will be greater, but the graph of changes in the calculated values will look smoother.

It is known [15] that for fixed distributions of the random variable  $X$  generating the series (1), the entropy is related to the standard deviation (SD)  $\sigma$  by certain dependence. For example, if a quantity  $X$  has a continuous normal distribution, then [16]

$$\begin{aligned} H &= -\int_{-\infty}^{+\infty} p(X) \log p(X) dX = -\int_{-\infty}^{+\infty} p(X) \left[ \log \frac{1}{\sqrt{2\pi}\sigma} - \frac{X^2}{2\sigma^2} \log e \right] dX = \\ &= -\log(\sqrt{2\pi}\sigma) \int_{-\infty}^{+\infty} p(X) dX + \frac{\log e}{2\sigma^2} \int_{-\infty}^{+\infty} p(X) X^2 dX = \log \sigma \sqrt{2\pi} + \frac{1}{2} \log e = \end{aligned}$$

$$= \log \sigma \sqrt{2\pi e} = 0.5 \log_2 2\pi e + \log_2 \sigma. \quad (13)$$

It follows that for a continuous normal distribution the relationship between  $H$  and  $\sigma$  is

$$H \cong 2.05 + \log_2 \sigma. \quad (14)$$

For experimental verification of this relationship, model experiments were carried out.

## MODEL EXPERIMENTS

The experiments were carried out by processing the generated test sequences of independent normally distributed quantities  $a_i$ ,  $i=1, \dots, N$  with zero mean and  $\sigma=0.1$  for different values of the number of points  $N$ . Following the recommendations of [17], to determine the boundaries (4), (5) of the intervals  $\Delta_j = [a_j^-, a_j^+]$ ,  $j=1, \dots, n$  the value was taken  $n=12$ .

Model experiments have shown that under  $N > 200$  the graphs of the theoretical and experimental dependences have almost the same form (Fig. 2).

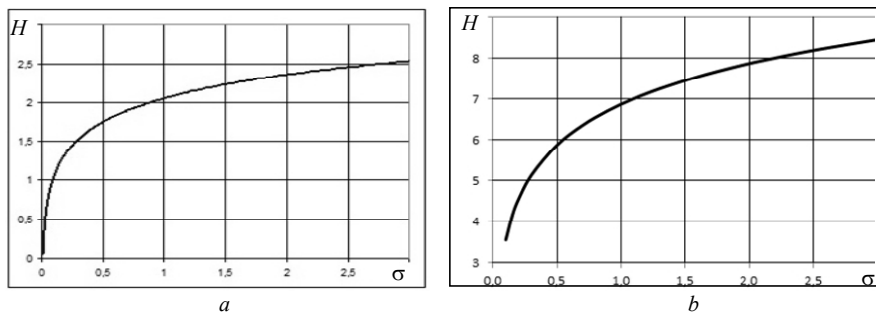
The nonlinear character of the dependences (14) leads us to the important conclusion. With a normal distribution of the random variable  $X$  that generates the sequence (1), even minor changes in the SD in the region of small values lead to large changes in the Shannon entropy, whereas a change of the same percentage in the region of large values practically does not lead to any changes in  $H$ .

It is easy to verify that the boundary of these regions determines the value of the SD

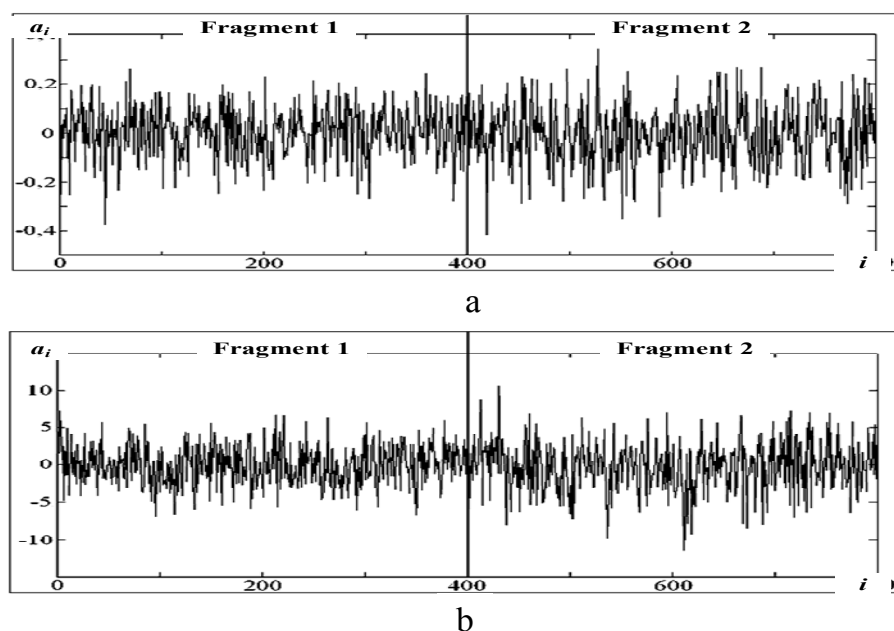
$$\sigma_0 \approx 1.443, \quad (15)$$

satisfying the condition  $\partial H / \partial \sigma = 1$ .

To illustrate, let us consider the results of estimating the chaoticity of two model signals, which are a sequence of independent normally distributed quantities with zero mean and different values of the SD at the first and second halves of the observations (Fig. 3).



**Fig. 2.** Graphs of the entropy  $H$  dependences on the SD  $\sigma$  under normal distribution: is the theoretical dependence (14); is the experimental dependence ( $N = 400$  points)



**Fig. 3.** Model signals with low (a) and high (b) values of SD

The first signal (Fig. 3, a) consists of two fragments of  $N = 400$  points each with the parameters  $\sigma_{11} = 0.1$  and  $\sigma_{12} = 0.13$ , respectively, and the second signal (Fig. 3, b) consists of two fragments of points  $N = 400$  with the parameters  $\sigma_{21} = 2.70$  and  $\sigma_{22} = 3.51$ , respectively. Thus, on the second halves of both signals, the same increase in SD is observed in comparison with the first half, equal to 30 %. But in this case the values of the SD on the first signal belong to the region  $\sigma < \sigma_0$ , and on the second signal — to the region  $\sigma > \sigma_0$ , where  $\sigma_0$  is the threshold value determined by the relation (15).

Table 1 presents the results of calculating the Shannon entropy on fragments of these series.

**Table 1. Results of modeling**

Test signal	SD, un.	SD increase	Entropy, un.	Entropy increase
Time series 1	0.1	30 %	1.90	20 %
	0.13		2.29	
Time series 2	2.7	30 %	4.93	2 %
	3.51		5.05	

Thus, with the same increment in the SD (30 %), the increment of the Shannon entropy on the second signal was lower than the first signal.

Let's make a comparative analysis of the estimating results of the dynamic

series variability using sliding windows. The model signal was a sequence of  $M=10$  fragments, each consisting of  $K_0=50$  dots and generated by an autoregressive model of the form

$$a_{kl} = \lambda_l a_{k-1,l} + (1 - \lambda_l) \xi_{k-1,l}, \quad k = 1, \dots, K_0, \quad l = 1, \dots, M, \tag{16}$$

where  $\lambda_l$  ( $0 < \lambda_l < 1$ ) is the parameter that determines the variability of the signal on the  $l$ -th fragment,  $a_{0l} = 0.1$  is the initial value,  $\xi \in N(0, \sigma^2)$  is a sequence of independent normally distributed random numbers with zero mathematical expectation and variance  $\sigma^2 = 3$ .

Thus, the entire signal contained  $N = 500$  points. The parameter values on the  $\lambda_1, \lambda_2, \dots, \lambda_{10}$  fragments of one of the test signals are presented in Table 2, and the graph of this signal is shown in Fig. 4.

Table 2. The values of the parameters  $\lambda_l$  on the test signal fragments

$l$	1	2	3	4	5	6	7	8	9	10
$\lambda_l$	0.93	0.86	0.75	0.1	0.2	0.3	0.6	0.7	0.8	0.9

The results of estimating the variability of the test signal using procedures (7) and (11) with sliding windows are shown in Fig. 5.

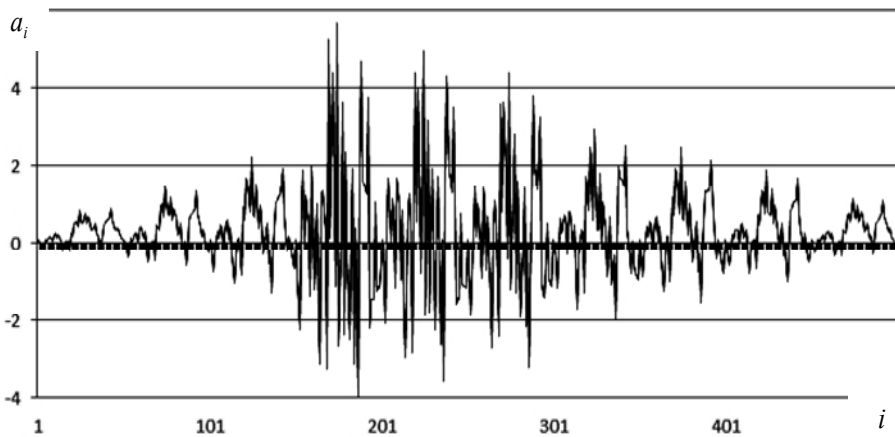
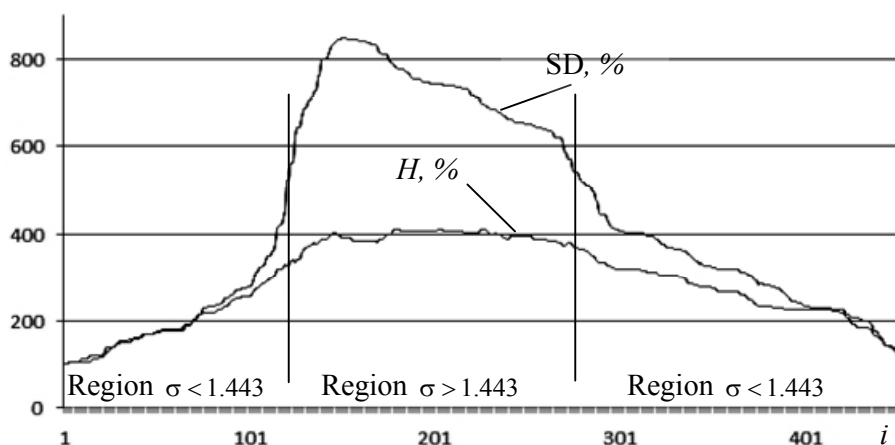


Fig. 4. The test signal of the 10 fragments with different parameters  $\lambda_l$





**Fig. 5.** Dynamics of changes in the SD and Shannon entropy  $H$  during the processing of the test signal

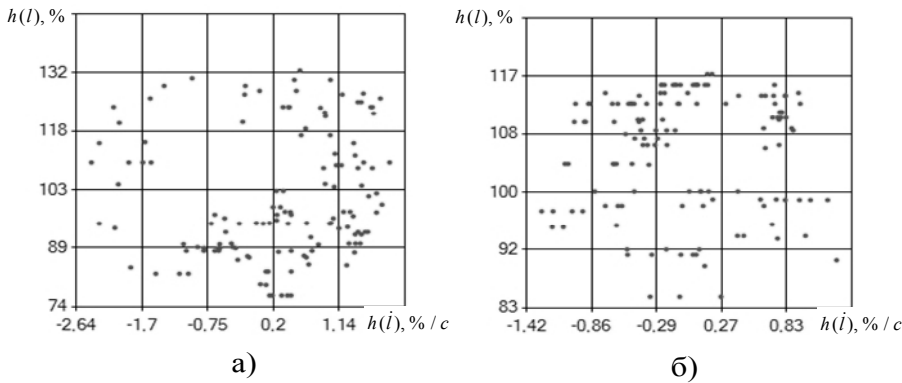
It is easy to see that both parameters had similar trends — an increase in SD was accompanied by an increase in entropy, and vice versa. But in the region  $\sigma > \sigma_0$ , the sensitivity of the entropy to the variability of the signal is almost 2 times less than the sensitivity of the SD, which agrees with the results of the study of the theoretical relationship between these values.

### PHASE PORTRAIT OF SLIDING ENTROPY

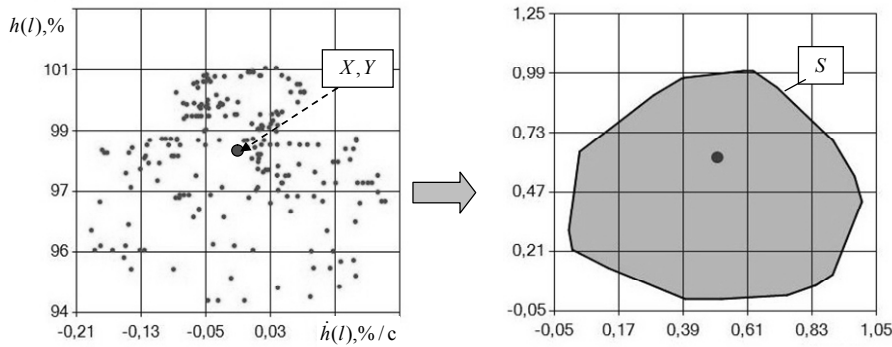
To increase the sensitivity of entropy assessment to the variability of the dynamic series, it is proposed to move from a series of discrete values  $h(l)$  calculated by the sliding window method to a phase portrait of entropy on the plane  $h(l), \dot{h}(l)$ , where  $\dot{h}(l)$  is the estimation of the first derivative  $h(l)$  at the  $l$ -th point.

Despite the fact that the procedure of numerical differentiation of noisy data refers to incorrectly posed mathematical problems, the application of special filtration and regularization procedures [18] allowed us to obtain acceptable estimates of the derivative  $\dot{h}(l)$ . As a result, it is possible to construct graphic images of the entropy phase portrait as points on the plane  $h(l), \dot{h}(l)$ .

For illustration, Fig. 6 shows examples of phase portraits of Shannon and permutation entropies, which are constructed from the same dynamic series of parameter  $\beta_T$  values (symmetry of the  $T$ -wave in the process of recording the electrocardiogram), which are used as an additional diagnostic sign of coronary heart disease in the method of phasegraphy [19].



**Fig. 6.** Phase portraits of the Shannon (a) and permutation (b) entropy of the parameter  $\beta_T$  on the real ECG



**Fig. 7.** The phase portrait of the sliding entropy (left) and its convex hull (right)

For an integral estimate of the physiological signals chaoticity, we construct in the normalized coordinates  $h(l), \dot{h}(l)$  the convex hull of the entropy phase portrait and determine the area  $S$  of the resulting polygon, as well as the coordinates  $X, Y$  of the phase portrait center of gravity (Fig. 7).

**PRACTICAL RESULTS**

A serious manifestation of cardiovascular disease is sudden cardiac death, when a patient dies almost instantaneously (from a few seconds to an hour) after the onset of a heart attack. One of the predictors of sudden cardiac death, which has recently gained wide popularity in clinical studies, is based on an analysis of the so-called electrical heart alternation [20], which refers to the regular alternation of the electrocardiogram elements characteristics.

The complexity of constructing computer algorithms for automatic detection of the alternation effect is due to the fact that real signals with the presence and absence of an electrical alternation are externally virtually indistinguishable (Fig. 8) [19].



**Fig. 8.** ECG with a random distortion (top) and *T*-wave alternation (bottom)

At the same time, the proposed method for estimating the randomness of the time sequence on the basis of calculating the area of the convex hull of the entropy phase portrait makes it possible to reliably solve this problem. To test the effectiveness of this method, test signals with different values of the *T*-wave amplitudes alternation levels were generated against a background of 15 % random distortions. Test signals were generated on the basis of the generative model of artificial realistic forms ECG generation [21].

Despite the fact that visually these signals were practically indistinguishable, the area of the convex hull of the permutation entropy phase portrait (EPP) decreased monotonically as the alternation of the *T*-wave increased, i.e. increasing proportion of the regular component of amplitude variation (Table 3). At the alternation level of 60 mV, the area decreased by more than 30 % (from 0.89 units to 0.62 units) compared to the signal without alternation.

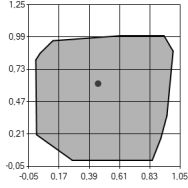
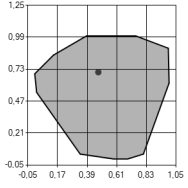
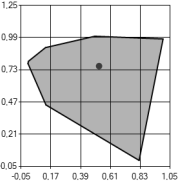
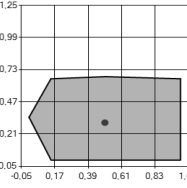
The proposed approach has also found practical application in assessing subtle changes in the signal during the intravenous therapy. The research was conducted in 2016 in the State Scientific Institution "Scientific and Practical Center for Preventive and Clinical Medicine" State Administration (SSI "SPC PCM" SA). The urgency of this task is due to the fact that many medications, including those used in cardiological practice, often have side effects (from 30 to 70 %) [22].

Table 4 shows the results of ECG treatment during the intravenous drip infusion of Tivomax, Armadin and T-triomax to a patient R. at the age of 72 years old with pronounced bigeminy, which manifested itself in the regular alternation of normal and extrasystolic heart cycles. ECG was recorded every 5 minutes during the introduction of medications. Each ECG was recorded for 150 seconds with a total duration of 2 hours.

As can be seen from the table, by the time of 12:03 (35 minutes after the start of the medication administration) the heart rate returned to normal, there was a sharp decrease (by 92 %) of the *SDNN* parameter, the traditional index of heart rate variability. At this point in time, the area  $S_{RR}$  of the permutation entropy phase portrait of the *RR*-intervals has decreased by 44 % from the initial value.

It should be noted that after the normalization of the rhythm during the further administration of medications, the parameter *SDNN* remained practically unchanged, while the area  $S_{RR}$  continued to decrease smoothly

Table 3. Areas of EPP convex hulls with a *T*-wave alternation

<i>T</i> -wave amplitude alternation level, mcV			
0	15	30	60
 $S = 0.89 \text{ un.}$	 $S = 0.76 \text{ un.}$	 $S = 0.64 \text{ un.}$	 $S = 0.62 \text{ un.}$

(Fig. 9). Since, as already noted, the Shannon entropy (unlike the SD) characterizes not the magnitude of the spread, but the variety of the processed sequence, such a gradual change in the parameter  $S_{RR}$  after restoration of the heart rhythm, that carries information on subtle changes in the heart rhythm, may have additional diagnostic value, which requires further study.

It is also clear that monitoring the ECG during the drip administration of drugs allows you to control the absence of undesirable changes in parameters caused by individual drug intolerance.

To illustrate such possibilities, Table 5 shows the dynamics of changes in the ECG parameters of patient I. 76 years old in the process of drip administration of Panangin and Mexicor medications. During the entire period of administration, the median ECG cycle in the time domain and in the phase plane remained practically unchanged, and the values of the *T*-wave symmetry parameter were within the physiological norm:  $\beta_T = 0.653 \pm 0.014$  units. Stable was the area of the EPP convex hull parameter  $\beta_T$ :  $S_{\beta_T} = 0.743 \pm 0.016$  units, which gave the reason for the doctors to continue treatment without changing the dosage of the medications.

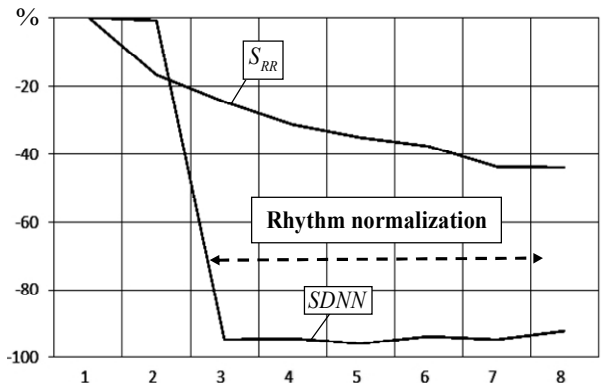


Fig. 9. Dynamics of changes in the integral heart rate parameters in the process of drip administration

Table 4. Dynamics of ECG parameters during patient R. dropper

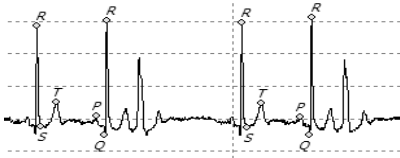
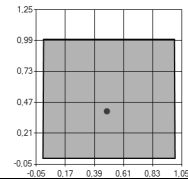
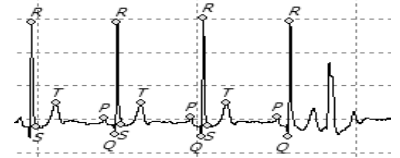
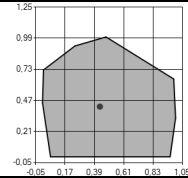

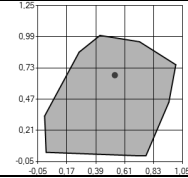
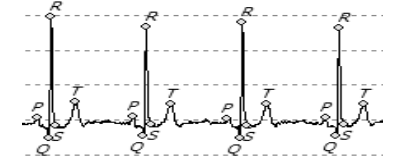
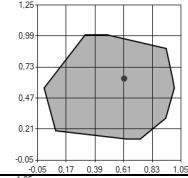
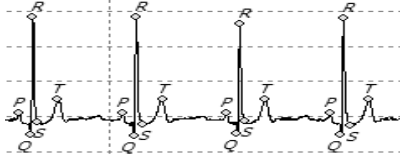
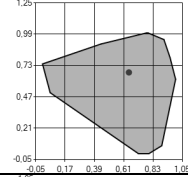

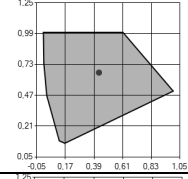
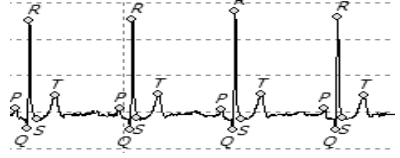
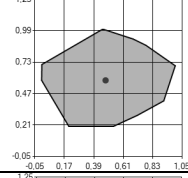
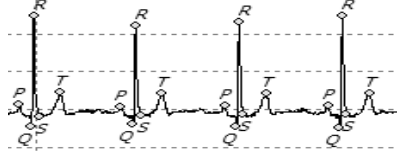
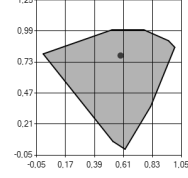
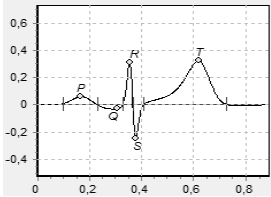
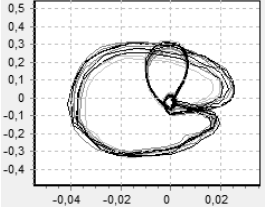
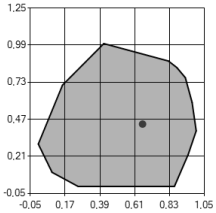
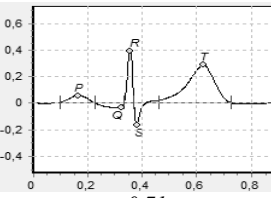
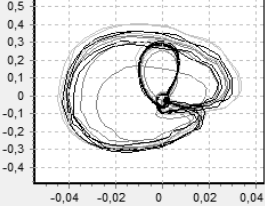
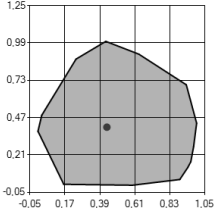
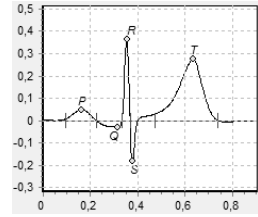
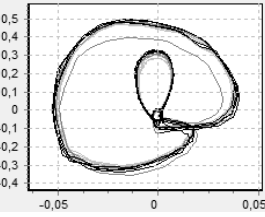
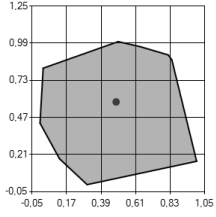
Recording time	ECG fragment	RR-intervals EPP	$S_{RR}$ , un.	SDNN, ms
11:35			0.995	515
11:47			0.83	510
12:03			0.751	27
12:12			0.682	30
12:32			0.644	22
12:37			0.619	33
12:47			0.561	27
13:02			0.555	41

Table 5. ECG parameters dynamics for drip administration of potassium medications

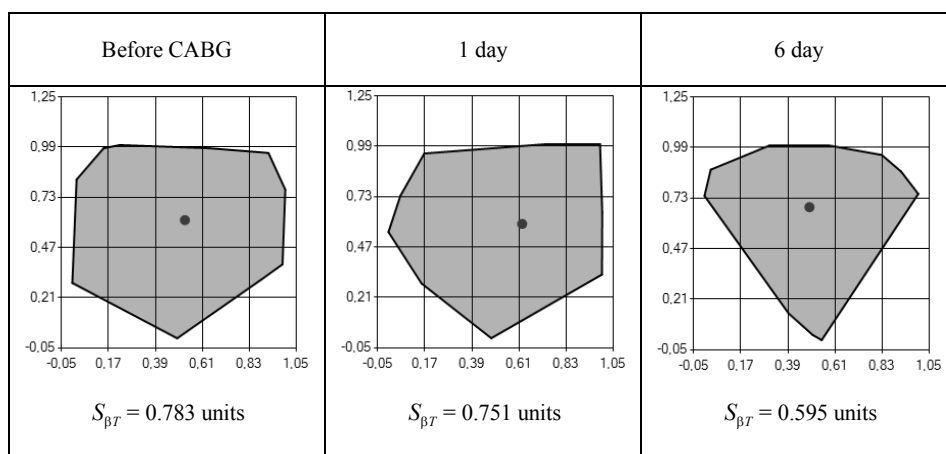
Ti me	Average cycle	ECG phase portrait	The EPP convex hull of the $\beta_T$
15 min	 $\beta_T = 0.65 \text{ un.}$	 $A_T = 0.44 \text{ mV}$	 $S_{\beta_T} = 0.764 \text{ un.}$
25 min	 $\beta_T = 0.71 \text{ un.}$	 $A_T = 0.29 \text{ mV}$	 $S_{\beta_T} = 0.754 \text{ un.}$
40 min	 $\beta_T = 0.64 \text{ un.}$	 $A_T = 0.28 \text{ mV}$	 $S_{\beta_T} = 0.744 \text{ un.}$

Interesting results were obtained in the study of subtle ECG changes by estimating the area of the convex hull of the permutation entropy phase portrait in patients with coronary heart disease that underwent coronary artery bypass surgery (CABG).

Since such an operation is most often performed in the open heart with the use of an artificial circulation device, the ECG was recorded before and after surgery (Table 6).

On the first day after the operation, the EPP  $\beta_T$  parameter decreased by 5 %, and on the 7-th day after the operation its value reached  $S_{\beta_T} = 0.595$ , which is 24 % lower than before surgery. The patient successfully passed the rehabilitation period and was discharged a week after the operation.

Of particular interest is the study of subtle ECG changes directly in the process of coronary stenting, which is more sparing surgical treatment for the patient, which, unlike CABG, does not require cardiac arrest. The results of such a study, obtained with the stenting of the anterior interventricular branch of the right coronary artery to patient I. 50 years old with the diagnosis of postinfarction atherosclerosis, are presented in Table 7.

**Table 6. Dynamics of integral ECG parameters of a 55 years old patient before and after CABG**

It can be seen from the table that the area of the Shannon entropy phase portrait of the  $\beta_T$  parameter increases during the whole procedure by 27 %, and on the next day after the operation by 33 %. The symmetry of the  $T$ -wave also increases during the entire operation, reaching 42 % when the blood flow of the anterior interventricular branch of the right coronary artery is restored. On the first day after stenting, the value of the symmetry index decreased to a physiological norm of  $\beta_T = 0.67$  units.

Similar results were observed when examining ECG changes during the installation of several stents (in the circumflex branch and in the anterior interventricular branch of the coronary artery) to a 74 years old patient diagnosed with stenosing coronary artery atherosclerosis (Table 8).

In this case, during the operation, the symmetry index of the  $T$ -wave was practically unchanged and was within the limits of the physiological norm:  $\beta_T = 0,64 \pm 0,09$  units. At the same time, the area of the phase portrait of the permutation entropy increased throughout the procedure, reaching 45 % by the end of the operation, and the control measurement for the following day showed a decrease in  $\beta_T$  EPP by 35 %.

We also note that during the operation a gradual decrease in the integral parameter  $Y_{\beta_T}$  (the center of gravity of the EPP along the y-axis) by the end of the operation reached 20 % of the initial value. This indicates that in this patient decreased average level entropy in the course of operations, which most likely indicated a lower level of adaptive capacity of the organism than a younger patient.

The detected fact made it possible to put forward the hypothesis that important additional diagnostic information in assessing the reserve capabilities of the cardiovascular system can provide an analysis of the ECG phase portrait during exercise. We present the first results aimed at studying such possibilities.

Table 7. Dynamics of changes in EPP parameter during stenting

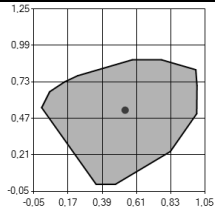
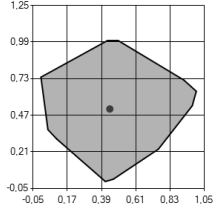
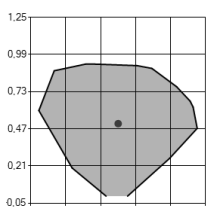
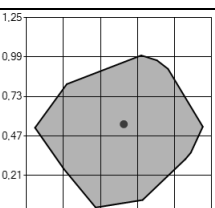
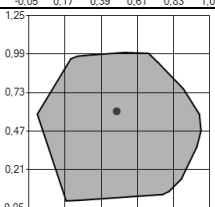
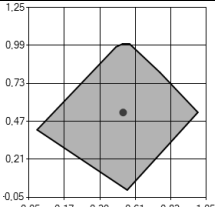
#	Phase	The convex hull of a $\beta_T$ EPP	Integral parameters
0	Baseline		$S_{\beta T} = 0.613 \text{ un.};$ $X_{\beta T} = 0.537 \text{ un.};$ $Y_{\beta T} = 0.528 \text{ un.};$ $\beta_T = 0.65 \text{ un.}$
1	Introduction of stent delivery catheter		$S_{\beta T} = 0.633 \text{ un.};$ $X_{\beta T} = 0.443 \text{ un.};$ $Y_{\beta T} = 0.514 \text{ un.};$ $\beta_T = 0.95 \text{ un.}$
2	Balloon inflating		$S_{\beta T} = 0.632 \text{ un.};$ $X_{\beta T} = 0.501 \text{ un.};$ $Y_{\beta T} = 0.506 \text{ un.};$ $\beta_T = 0.97 \text{ un.}$
3	Restoration of the blood flow of the anterior interventricular branch of the right coronary artery		$S_{\beta T} = 0.645 \text{ un.};$ $X_{\beta T} = 0.529 \text{ un.};$ $Y_{\beta T} = 0.548 \text{ un.};$ $\beta_T = 0.92 \text{ un.}$
4	Introduction of nitrates		$S_{\beta T} = 0.776 \text{ un.};$ $X_{\beta T} = 0.485 \text{ un.};$ $Y_{\beta T} = 0.604 \text{ un.};$ $\beta_T = 0.77 \text{ un.}$
5	1 day after stenting		$S_{\beta T} = 0.521 \text{ un.};$ $X_{\beta T} = 0.535 \text{ un.};$ $Y_{\beta T} = 0.53 \text{ un.};$ $\beta_T = 0.67 \text{ un.}$



Table 8. Dynamics of changes in EPP parameters during stenting

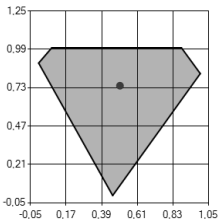
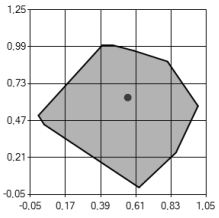
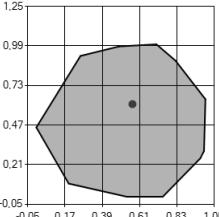
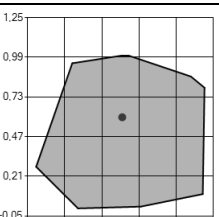
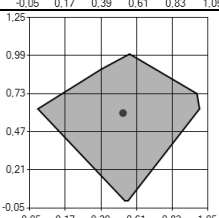
#	Stage	The convex hull of a $\beta_T$ EPP	Integral parameters
0	Baseline		$S_{\beta T} = 0.557 \text{ un.};$ $X_{\beta T} = 0.503 \text{ un.};$ $Y_{\beta T} = 0.743 \text{ un.};$ $\beta_T = 0.713 \text{ un.}$
1	Introduction of the introdu- cer		$S_{\beta T} = 0.597 \text{ un.};$ $X_{\beta T} = 0.56 \text{ un.};$ $Y_{\beta T} = 0.632 \text{ un.};$ $\beta_T = 0.644 \text{ un.}$
2	Reintroduction of introducer		$S_{\beta T} = 0.755 \text{ un.};$ $X_{\beta T} = 0.568 \text{ un.};$ $Y_{\beta T} = 0.608 \text{ un.};$ $\beta_T = 0.68 \text{ un.}$
3	Pain in the sternum, the introduction of an iso-mic spray		$S_{\beta T} = 0.81 \text{ un.};$ $X_{\beta T} = 0.511 \text{ un.};$ $Y_{\beta T} = 0.597 \text{ un.};$ $\beta_T = 0.526 \text{ un.}$
4	1 day after stenting		$S_{\beta T} = 0.529 \text{ un.};$ $X_{\beta T} = 0.527 \text{ un.};$ $Y_{\beta T} = 0.597 \text{ un.};$ $\beta_T = 0.732 \text{ un.}$

Table 9 shows the results obtained when testing a conditionally healthy 55 years old volunteer on a treadmill. During testing, the speed of the tape reached 2.7 km/h, and the angle of inclination gradually increased to 10 %, which in the second stage ensured the metabolic equivalent  $\text{MET} = 4.6$ . After that, the tested person rested for 10 minutes.

In the process of increasing the load, the  $SDNN$  parameter decreased by 86 %, which agrees with the known data on the increase in the sympathetic part

of the autonomic nervous system under load. Simultaneously with the decrease in heart rate variability, the integral parameter  $S_{RR}$  characterizing the area of the convex hull of the permutation entropy phase portrait increased by 66 %. Recall that, unlike  $SDNN$ , this parameter characterizes not the degree of dispersion, but the variety of  $RR$ -intervals.

It is clear that load tests using treadmill and veloergometer can be used only in medical conditions. Such tools are of little use for testing in the field, in sports, in the workplace, etc. This requires not only portable ECG measurement tools, but also simple methods that allow to obtain operational test results in a convenient and understandable form.

In this regard, it is of interest to evaluate the possibilities of the proposed approach when performing simplified methods for assessing the adaptive capacity of a person under stress, in particular, the famous Martine-Kushelevsky test. To perform such studies, it is sufficient to estimate the EPP parameters in three states: before the stress, after performing 20 deep sit-ups in 30 seconds and during restitution period after 3 min rest.

During the studies, ECG treatment was performed on 30 healthy volunteers at the age of  $20,6 \pm 1$  year. For illustration, Table 10 shows the results obtained with the testing of volunteer M. 20 years old.

As follows from the data given at the height of the load, the  $SDNN$  parameter (SD of the  $RR$ -intervals) decreased by 18 %, while the  $S_{RR}$  area increased by 12 %. There were also characteristic changes in the integral parameters  $X_{RR}$  and  $Y_{RR}$ : the EPP center of gravity shifted to the left by 24 % of the initial value and rose by 34 %.

**Table 9. Dynamics of changes in integral parameters for a treadmill test**

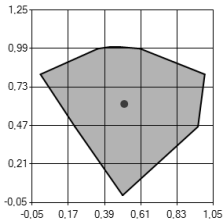
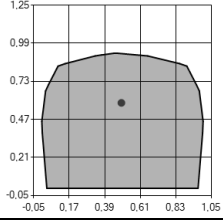
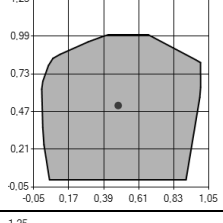
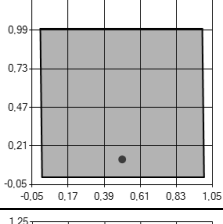
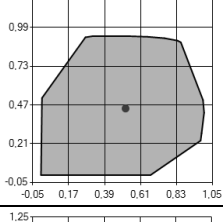
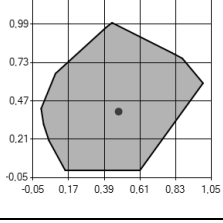
#	Stage	MET	The convex hull of a RR-intervals EPP	Integral parameters
0	Baseline	1		$S_{RR} = 0.593 \text{ un.};$ $X_{RR} = 0.51 \text{ un.};$ $Y_{RR} = 0.616 \text{ un.};$ $SDNN = 135 \text{ ms}$
1	3 min stress	2.3		$S_{RR} = 0.837 \text{ un.};$ $X_{RR} = 0.494 \text{ un.};$ $Y_{RR} = 0.583 \text{ un.};$ $SDNN = 99 \text{ ms}$
2	6 min stress	3.5		$S_{RR} = 0.888 \text{ un.};$ $X_{RR} = 0.481 \text{ un.};$ $Y_{RR} = 0.512 \text{ un.};$ $SDNN = 90 \text{ ms}$
3	9 min stress	4.6		$S_{RR} = 0.989 \text{ un.};$ $X_{RR} = 0.5 \text{ un.};$ $Y_{RR} = 0.12 \text{ un.};$ $SDNN = 18 \text{ ms}$
4	3 min rest	-		$S_{RR} = 0.79 \text{ un.};$ $X_{RR} = 0.518 \text{ un.};$ $Y_{RR} = 0.446 \text{ un.};$ $SDNN = 94 \text{ ms}$
5	6 min rest	-		$S_{RR} = 0.667 \text{ un.};$ $X_{RR} = 0.478 \text{ un.};$ $Y_{RR} = 0.398 \text{ un.};$ $SDNN = 89 \text{ ms}$

Table 10. Dynamics of EPP *RR*-intervals of a healthy volunteer M.

Before stress	Stress	Restitution
 $S_{RR} = 0.65 \text{ un.};$ $X_{RR} = 0.497 \text{ un.};$ $Y_{RR} = 0.501 \text{ un.};$ $SDNN = 69 \text{ ms}$	 $S_{RR} = 0.729 \text{ un.};$ $X_{RR} = 0.408 \text{ un.};$ $Y_{RR} = 0.695 \text{ un.};$ $SDNN = 54 \text{ ms}$	 $S_{RR} = 0.662 \text{ un.};$ $X_{RR} = 0.38 \text{ un.};$ $Y_{RR} = 0.671 \text{ un.};$ $SDNN = 95 \text{ ms}$

A similar reaction to the load was demonstrated by 12 other volunteers. This result shows once again that the *SDNN* and *S<sub>RR</sub>* parameters from different perspectives characterize the variability of the heart rhythm: the first parameter characterizes only the magnitude of the *RR*-intervals spread, and the second parameter characterizes the variety of their values.

CONCLUSIONS

The article considers various approaches to the assessment of heart rate variability and other parameters of a single-channel ECG under the effect of external influences on the body (intravenous therapy, surgery and physical activity). A comparative analysis of two approaches to the variability estimation is carried out: based on the dispersion analysis and the Shannon entropy calculated from successive sections of the same discrete signal.

To increase the Shannon entropy sensitivity to an estimation of a variety of an investigated parameter in the course of its observation, it is proposed to construct an entropy phase portrait calculated in a sliding window and to estimate the area of its convex hull and the coordinates of the gravity center in the phase plane.

Characteristic changes in these integral parameters are established when the effect of electrical alternation of the heart is detected, as well as during physical exertion (treadmill and Martine-Kushelevsky test), with drip administration of medications and in operative treatment of cardiovascular pathologies (coronary artery bypass surgery and stenting).

It can be assumed that the detected facts of changes in the values of the proposed integral indicators of the entropy phase portrait, including the *S<sub>RR</sub>* parameter, indicate the search for the most economical way of regulating cardiac activity. Of course, such a hypothesis requires further study and evaluation of the statistical reliability of the observed differences in representative samples of

observations, which can lay the basis for new diagnostic criteria in preventive and clinical cardiology.

## REFERENCES

1. Klimontovich Yu.L. Introduction to physics of open systems. Moscow: Janus-K; 2002. 284 p.
  2. Martin-Sanchez F., Iakovidis I., Nørager S., Maojo V., de Groen P., Van der Lei J., Jones T., Abraham-Fuchs K., Apweiler R., Babic A., Baud R., Breton V. Synergy between medical informatics and bioinformatics: facilitating genomic medicine for future health care. *Journal of Biomedical Informatics*. 2004. Vol. 37. N 1. P. 30–42.
  3. Weippert M., Behrens M., Rieger A., Behrens K. Sample entropy and traditional measures of heart rate dynamics reveal different modes of cardiovascular control during low intensity exercise. *Entropy*. 2014. Vol. 16. P. 5698–5711.
  4. Durnova N.Yu., Dovgalevskiy Ya.P., Burlaka A.N., Kiselev A.R., Furman N.V. Interdependence of parameters of variational pulsometry, entropy of heart rate, temporal and spectral analyses of heart rate variability in normal state and in ischemic heart disease. *Saratov journal of medical scientific research*. 2011. Vol. 7. N 3. P. 607–611.
  5. Ban A.S., Paramonova N.A., Zagorodnyy G.M., Ban D.S. Analysis of the relationship of heart rate variability indices. *Voennaya Meditsina*. 2010. N 4. P. 21–24.
  6. Joshua S., Richman J., Moorman R. Physiological time-series analysis using approximate entropy and sample entropy. *The American journal of physiology*. 2000. Vol. 278. N 6. P. 2039–2049.
  7. Peng C.K., Havlin S., Stanley H.E., Goldberger A.L. Quantification of scaling exponents and crossover phenomena in nonstationary heartbeat time series. *Chaos*. 1995. Vol. 5. P. 82–87.
  8. Iyengar N., Peng C.K., Morin R., Goldberger A.L., Lipsitz L.A. Age-related alterations in the fractal scaling of cardiac interbeat interval dynamics. *Am. J. Physiol.* 1996. Vol. 271. P. 1078–1084.
  9. Mayorov O.Yu., Fenchenko V.N. Calculation of the correlation dimension and entropy of EEG signals in cluster computing systems. *Clinical informatics and telemedicine*. 2014. Vol. 10. N 11. P. 10–20.
  10. Anishchenko V.S., Saparin P.I. Normalized entropy as a diagnostic criterion of human cardio-vascular system reaction on the external influence. *Izvestia VUZ. Applied nonlinear dynamics*. 1993. Vol. 1. N 3–4. P. 54–64.
  11. Shapovalov V.I. About the fundamental laws of trend management. *Control Science*. 2005. Vol. 2. P. 2–11.
  12. Yashin A.A. Living matter. Physics of the alive and evolutionary processes. Moscow: LKI, 2010. 264 p.
  13. Zhukovska O.A., Glushauskene G.A., Fainzilberg L.S. Research of the modified estimation properties of random variable's variance on sample of different observations. *Naukovi Visti NTUU KPI*. 2008. N 4. P. 139–145.
  14. Fainzilberg L.S., Orikhovska K.B., Vakhovskiy I.V. Assessment of chaotic fragments' shape of the single-channel electrocardiogram. *Cybernetics and computer engineering*. 2016. Vol. 183. P. 4–24.
  15. Gorban I.I. Entropy of uncertainty. *Mathematical Machines and Systems*. 2013. N 2. P. 105–117.
  16. Afanasyev V.V. Theory of Probability: a textbook for university students studying in the specialty "Mathematics". M.: The Humanitarian publishing center VLADOS, 2007. 350 p.
  17. Kramarenko S.S. Method of use of the entropy-information analysis for quantitative attributes. *Proceedings of the Samara Scientific Center of the RAS*. 2005. Vol. 7. N 1. P. 242–247.
  18. Fainzilberg L.S. Information technology for signal processing of complex shape. Theory and practice. Kiev: Naukova Dumka, 2008. 333 p.
- ISSN 2519-2205 (Online), ISSN 0454-9910 (Print). Киб. и выч. техн. 2017. № 3 (189)

19. Fainzilberg L.S. *Fasegraphy basics*. Kyiv: Osvita Ukrainy, 2017. 264 p.
20. Rosenbaum D.S., Jackson L.E., Smith J.M. Electrical alternans and vulnerability to ventricular arrhythmias. *New England Journal of Medicine*. 1994. Vol. 330. P. 235–241.
21. Fainzilberg L.S., Bekler T.Yu. T-Wave Alternans Modeling on artificial electrocardiogram with internal and external perturbation. *Journal of Automation and Information Sciences*. 2012. Vol. 44. N 7. P. 1–14.
22. Vlasova I.V. There are more and more side effects in drugs. *Commercial biotechnology*. 2007. Vol. 10. P. 14–19.

Received 5.06.2017

## ЛИТЕРАТУРА

1. Климонтович Ю.Л. Хаос и порядок. Эволюция. Деградация и самоорганизация. Москва: Янус-К, 2002. 284 с.. URL: [http://kirsoft.com.ru/freedom/KSNews\\_417.htm](http://kirsoft.com.ru/freedom/KSNews_417.htm)
2. Martin-Sanchez F., Iakovidis I., Nørager S., Maojo V., de Groen P., Van der Lei J., Jones T., Abraham-Fuchs K., Apweiler R., Babic A., Baud R., Breton V. Synergy between medical informatics and bioinformatics: facilitating genomic medicine for future health care. *Journal of Biomedical Informatics*. 2004. Vol. 37. Iss. 1. P. 30–42.
3. Weippert M., Behrens M., Rieger A., Behrens K. Sample Entropy and Traditional Measures of Heart Rate Dynamics Reveal Different Modes of Cardiovascular Control During Low Intensity Exercise. *Entropy*. 2014. Vol. 16. P. 5698–5711.
4. Дурнова Н.Ю., Довгалецкий Я.П., Бурлака А.Н., Киселев А.Р., Фурман Н.В. Изучение зависимостей между показателями вариационной пульсометрии, энтропии ритма сердца, временного и спектрального анализов variability ритма сердца в норме и при ишемической болезни сердца. *Саратовский научно-медицинский журнал*. 2011. Т. 7. № 3. С. 607–611.
5. Бань А.С., Парамонова Н.А., Загородный Г.М., Бань Д.С. Анализ взаимосвязи показателей variability ритма сердца. *Военная медицина*. 2010. № 4. С. 21–24.
6. Joshua S., Richman J., Moorman R. Physiological time-series analysis using approximate entropy and sample entropy. *The American journal of physiology*. 2000. Vol. 278. Iss. 6. P. 2039–2049.
7. Peng C.K., Havlin S., Stanley H.E., Goldberger A.L. Quantification of scaling exponents and crossover phenomena in nonstationary heartbeat time series. *Chaos*. 1995. Vol. 5. P. 82–87.
8. Iyengar N., Peng C.K., Morin R., Goldberger A.L., Lipsitz L.A. Age-related alterations in the fractal scaling of cardiac interbeat interval dynamics. *Am. J. Physiol.* 1996. Vol. 271. P. 1078–1084.
9. Майоров О.Ю., Фенченко В.Н. Вычисление корреляционной размерности и энтропии ЭЭГ сигналов на кластерных вычислительных системах. *Клиническая информатика и телемедицина*. 2014. Т. 10. Вып. 11. С. 10–20.
10. Анищенко В.С., Сапарин П.И. Нормированная энтропия как диагностический признак реакции сердечно-сосудистой системы человека на внешнее воздействие. *Изв. вузов. Прикладная нелинейная динамика*. 1993. Т. 1. № 3–4. С. 54–64.
11. Шаповалов В.И. О фундаментальных закономерностях управления тенденциями. *Проблемы управления (Control Science)*. 2005. № 2. С. 2–11.
12. Яшин А.А. Живая материя. Физика живого и эволюционных процессов. М.: ЛКИ, 2010. 264 с.
13. Жуковська О.А., Глушаускене Г.А., Файнзильберг Л.С. Дослідження властивостей модифікованої оцінки дисперсії випадкової величини за вибіркою незалежних спостережень. *Наукові вісті НТУ України КПІ*. 2008. № 4. С. 139–145.
14. Файнзильберг Л.С., Ориховская К.Б., Ваховский И.В. Оценка хаотичности формы фрагментов одноканальной ЭКГ. *Кибернетика и вычислительная техника*. 2016. Вып. 183. С. 4–24.
15. Горбань И.И. Энтропия неопределенности. *Математические машины и системы*. 2013. № 2. С. 105–117.

16. Афанасьев В.В. Теория вероятностей: учеб. пособие для студентов вузов, обучающихся по специальности «Математика». М.: Гуманитар. изд. центр ВЛАДОС, 2007. 350 с.
17. Крамаренко С.С. Особенности использования энтропийно-информационного анализа для количественных признаков биологических объектов. *Изв. Самар. Науч. Центра РАН*. 2005. Т. 7. № 1. С. 242–247.
18. Файнзильберг Л.С. Информационные технологии обработки сигналов сложной формы. Теория и практика. Киев: Наукова Думка, 2008. 333 с.
19. Файнзильберг Л.С. Основы фазографии. Киев: Освита Украины, 2017. 264 с.
20. Rosenbaum D.S., Jackson L.E., Smith J.M. Electrical alternans and vulnerability to ventricular arrhythmias. *New England Journal of Medicine*. 1994. Vol. 330. P. 235–241.
21. Fainzilberg L.S., Bekler T.Yu. T-Wave Alternans Modeling on Artificial Electrocardiogram with Internal and External Perturbation. *Journal of Automation and Information Sciences*. 2012. Vol. 44. Iss. 7. P. 1–14.
22. Власова И.В. У лекарств обнаруживается все больше побочных эффектов. *К Коммерческая биотехнология*. 2007. № 10. С.14–19.

К.Б. Ориховская, младш. науч. сотр., аспирант  
отд. интеллектуальных автоматических систем  
e-mail: kseniaor@gmail.com

Л.С. Файнзильберг, д-р техн. наук, доцент, глав. науч. сотр.  
отд. интеллектуальных автоматических систем  
e-mail: fainzilberg@gmail.com

Международный научно-учебный центр информационных технологий и систем  
НАН Украины и МОН Украины, пр. Академика Глушкова, 40,  
г. Киев, 03680, Украина

## СРАВНИТЕЛЬНЫЙ АНАЛИЗ МЕТОДОВ ОЦЕНКИ ИЗМЕНЧИВОСТИ ФИЗИОЛОГИЧЕСКИХ СИГНАЛОВ

*Введение.* В современном мире все большее внимание уделяется изучению поведения сложноорганизованных систем, к которым в первую очередь относятся медико-биологические системы. Фундаментальное понятие синергетики – обобщенная энтропия, которая количественно характеризует степень хаотичности системы. Особый интерес представляют исследования изменений показателей хаотичности динамических рядов, порождаемых различными биологическими системами.

*Цель статьи* – дальнейшее развитие и экспериментальное исследование математических методов оценки изменчивости физиологических сигналов при внешних воздействиях на организм.

*Методы.* Исследовано два альтернативных подхода оценки изменчивости динамических рядов: на основе вычисления относительных изменений выборочной дисперсии и энтропийных оценок (в скользящем окне с заданными параметрами) по отношению к первому (опорному) окну. Изучена теоретическая и экспериментальная зависимость между шенноновской энтропией и среднеквадратическим отклонением при нормальном распределении случайной величины, порождающей динамический ряд. Проведено сравнения указанных оценок на реальных и модельных данных.

*Результаты.* Для повышения чувствительности энтропийных оценок к изменчивости динамического ряда предлагается перейти от ряда дискретных значений энтропии  $h(l)$  в  $l$ -й точке, вычисленной методом скользящего окна, к ее фазовому портрету на плоскости  $h(l), \dot{h}(l)$ , где  $\dot{h}(l)$  – оценка первой производной  $h(l)$ . Для интегральной оценки хаотичности физиологических сигналов предложено оценить площадь выпуклой оболочки фазового портрета энтропии и координаты центра тяжести  $X, Y$  фазового портрета. Экспериментальные исследования подтвердили диагностическую ценность указанных показателей при оценке изменчивости параметров электрокардио-

ISSN 2519-2205 (Online), ISSN 0454-9910 (Print). Киб. и выч. техн. 2017. № 3 (189) 27

грамм и ритмограмм при внешних воздействиях на организм (введение лекарственных препаратов, оперативное вмешательство и физическая нагрузка).

**Выводы.** Обнаруженные отклонения интегральных показателей фазового портрета энтропии под действием внешних воздействий на организм открывают новые возможности в оценке регуляции сердечной деятельности в профилактической и клинической медицине и требуют дальнейшего изучения для подтверждения их статистической значимости на репрезентативных выборках наблюдений.

**Ключевые слова:** *изменчивость физиологических сигналов, энтропийные оценки, диагностические критерии.*

*К.Б. Ореховська*, молодш. наук. співроб., аспірант  
відд. відд. інтелектуальних автоматичних систем  
e-mail: kseniaor@gmail.com

*Л.С. Файнзильберг*, д-р техн. наук, доцент, голов. наук.  
співроб. відд. інтелектуальних автоматичних систем  
e-mail: fainzilberg@gmail.com  
Міжнародний науково-учбовий центр інформаційних технологій  
та систем НАН України та МОН України, пр. Академіка Глушкова, 40,  
м. Київ, 03680, Україна

#### ПОРІВНЯЛЬНИЙ АНАЛІЗ МЕТОДІВ ОЦІНЮВАННЯ МІНЛИВОСТІ ФІЗІОЛОГІЧНИХ СИГНАЛІВ

Розглянуто різні підходи до оцінки мінливості серцевого ритму та інших показників одно каналної ЕКГ під дією зовнішніх впливів на організм. Запропоновано новий підхід до оцінювання мінливості фізіологічних сигналів на основі визначення площі опуклої оболонки фазового портрета ковзної ентропії. Наведено результати застосування запропонованого підходу на модельних та реальних даних, зокрема для виявлення ефекту електричної альтернації серця, фізичному навантаженні (тредміл і проба Мартіна-Кушелевського), при краплинному введенні лікарських препаратів і при оперативному лікуванні серцево-судинних патологій (аортокоронарне шунтування та стентування).

**Ключові слова:** *мінливість фізіологічних сигналів, ентропійні оцінки, діагностичні критерії.*